# Supplementary Information

Glycogen Metabolism of the Anammox Bacterium "*Candidatus* Brocadia sinica"

By

Satoshi Okabe [1,*] Amrini Amalia Shafdar [1], Kanae Kobayashi [1], Lei Zhang [1] and Mamoru Oshiki [1]

[1] Division of Environmental Engineering, Faculty of Engineering, Hokkaido University, North-13, West-8, Kita-ku, Sapporo Hokkaido 060-8628, Japan

Supplementary information contains 1 Texts, 8 Figures, and 9 Tables.

**Bacterial glycogen synthesis pathways**

The GlgC-GlgA pathway has been known as the classical glycogen pathway. In this pathway glycogen is synthesized from glucose-1-phosphate (Glc-1P) by three enzyme actions catalyzed by glucose-1-phosphate adenylyltransferase (GlgC), glycogen synthase (GlgA) and glycogen branching enzyme (GlgB) (reviewed by Preiss, 2006). The Rv3032 pathway is associated with methylglucose lipopolysaccharide biosynthesis (Jackson and Brennan, 2009). Glucose-1-phosphate is also a primary substrate of glycogen in this pathway. An alternative branching enzyme (Rv3031) catalyzes formation of branched glucan chains having α-l,6-glucosidic linkages. In contrast, the GlgE pathway utilizes a disaccharide phosphate (maltose 1-phosphate) as the building block (Kalscheuer *et al*., 2010). Maltose 1-phosphate is generated from trehalose in two steps catalyzed by Maltose α-glucosyltransferase/α-amylase (TreS) and maltokinase (Pep2). On the other hand, glycogen is degraded to glucose-1-phosphate by debranching enzyme (GlgX) and glycogen phosphorylase (GlgP) or to trehalose via the (TreX)-TreY-TreZ pathway (Chandra *et al*., 2011).

**References**


1. Chandra, G., Chater, K. F., and Bronemann, S. (2011) Unexpected and widespread connections between bacterial glycogen and trehalose metabolism. *Microbiol* **157**: 1565-1572.
2. Jackson, M., and Brennan, P.J. (2009) Polymethylated polysaccharides from mycobacterium species revisited. *J Biol Chem* **284**: 1949-1953.
3. Kalscheuer, R., Syson, K., Veeraraghavan, U., Weinrick, B., Biermann, K. E., Liu, Z., Sacchettini, J.C., Besra, G., Bornemann, S., and Jacobs, W. R., Jr. (2010) Self-poisoning of Mycobacterium tuberculosis by targeting GlgE in an α-glucan pathway. *Nat Chem Biol* **6**: 376-384.
4. Preiss, J. (2006) Bacterial glycogen inclusions: enzymology and regulation of synthesis. *In* Microbiology Monographs, pp. 71-108. Edited by J. M. Shively. Heidelberg, Germany, Springer.

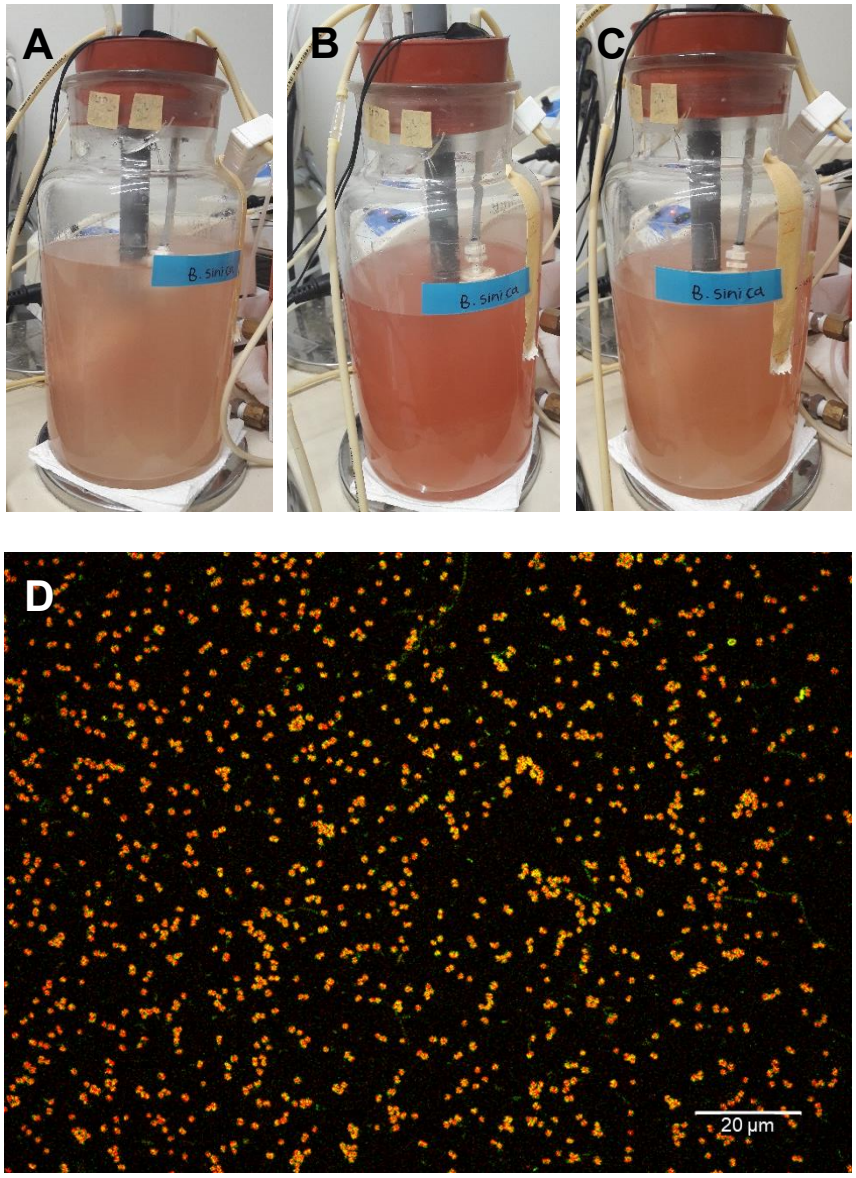


**Figure S1**. "*Ca.* B. sinica" culture in the membrane bioreactor (MBR) during growing phase (**A**), near-zero growth phase (**B**), and starvation phase (**C**), respectively. (**D**) FISH image of the MBR culture showing free-living planktonic cells of "*Ca.* B. sinica" after hybridization with Alexa555-labeled probe AMX820 and Alexa488-labeled probes EUB338, EUB338II and EUB338III (bacterial universal probes). "*Ca.* B. sinica" made up more than 96% of total population. Scale represents 20 μm.

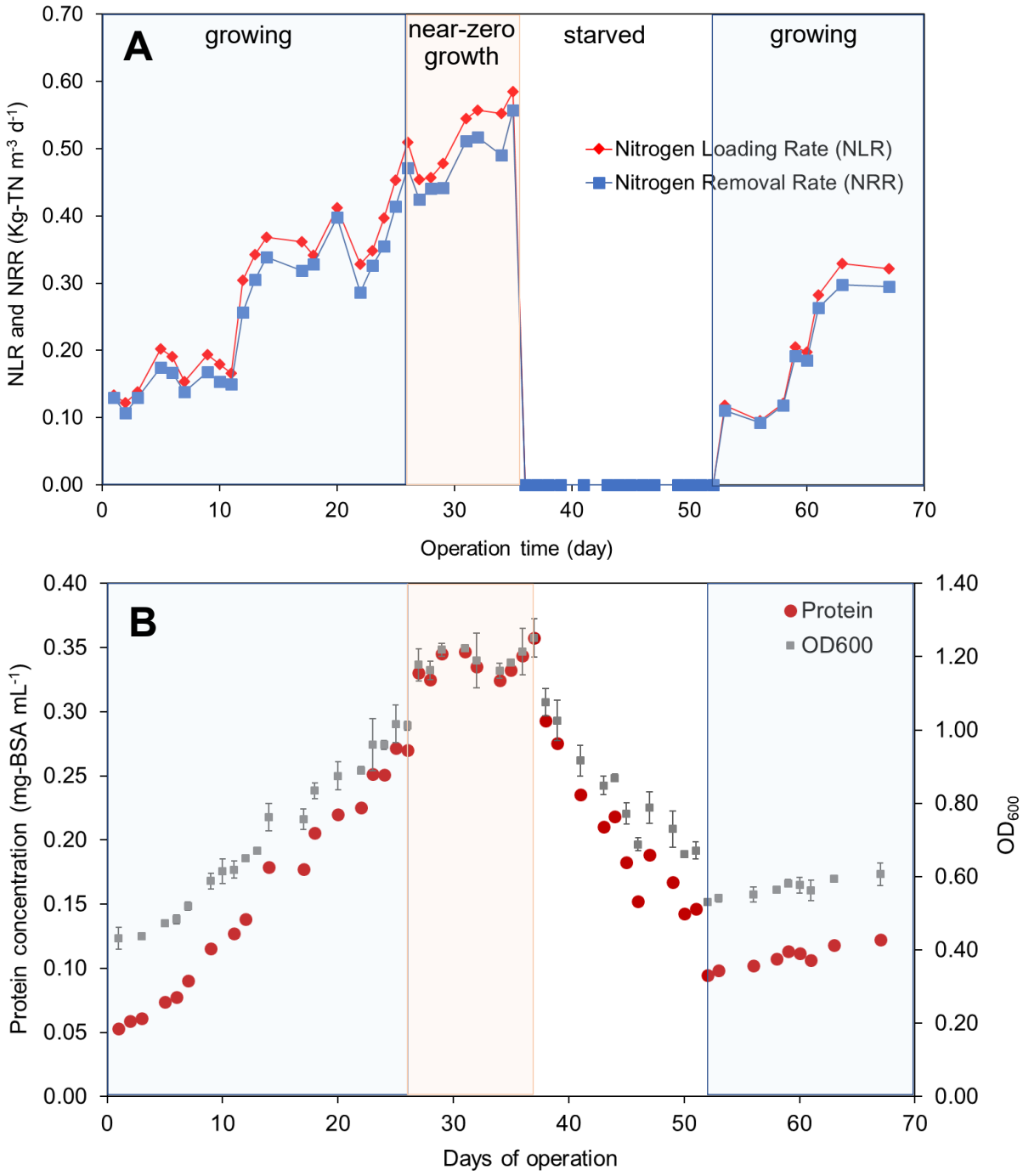


**Figure S2**. Time course of nitrogen ($NH_4^+$ and $NO_2^-$) loading rate (NLR) and removal rate (NRR) (**A**) and biomass concentration (protein and $OD_{600}$) (**B**) in a MRB during approx.70 days of continuous operation (Experimental Run-1). Blue, orange, and white area indicate the growing phase, near-zero growth phase, and starved phase, respectively. The error bars show SD of duplicate measurement.

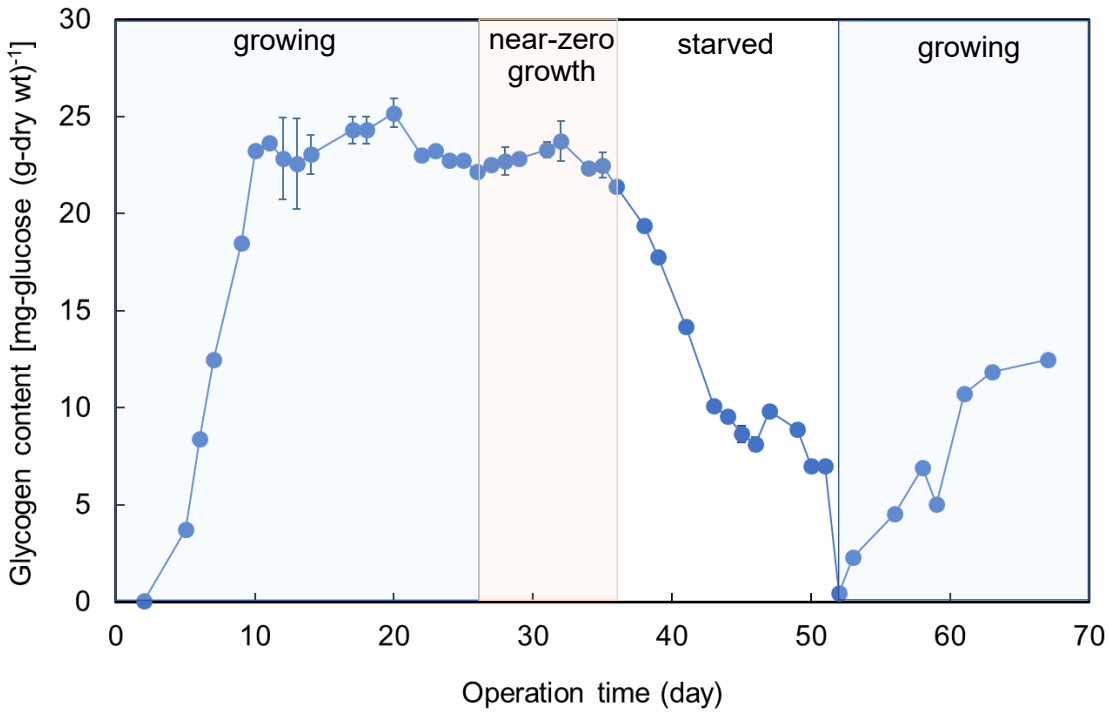


**Figure S3.** Change in intracellular glycogen content in "*Ca*. B. sinica" with time (Experimental Run-1). Glycogen accumulation was immediately observed when the substrate supply was resumed after 16-day starvation. Blue, orange, and white area indicate the growing phase, near-zero growth phase, and starved phase, respectively. The error bars show SD of duplicate measurement.

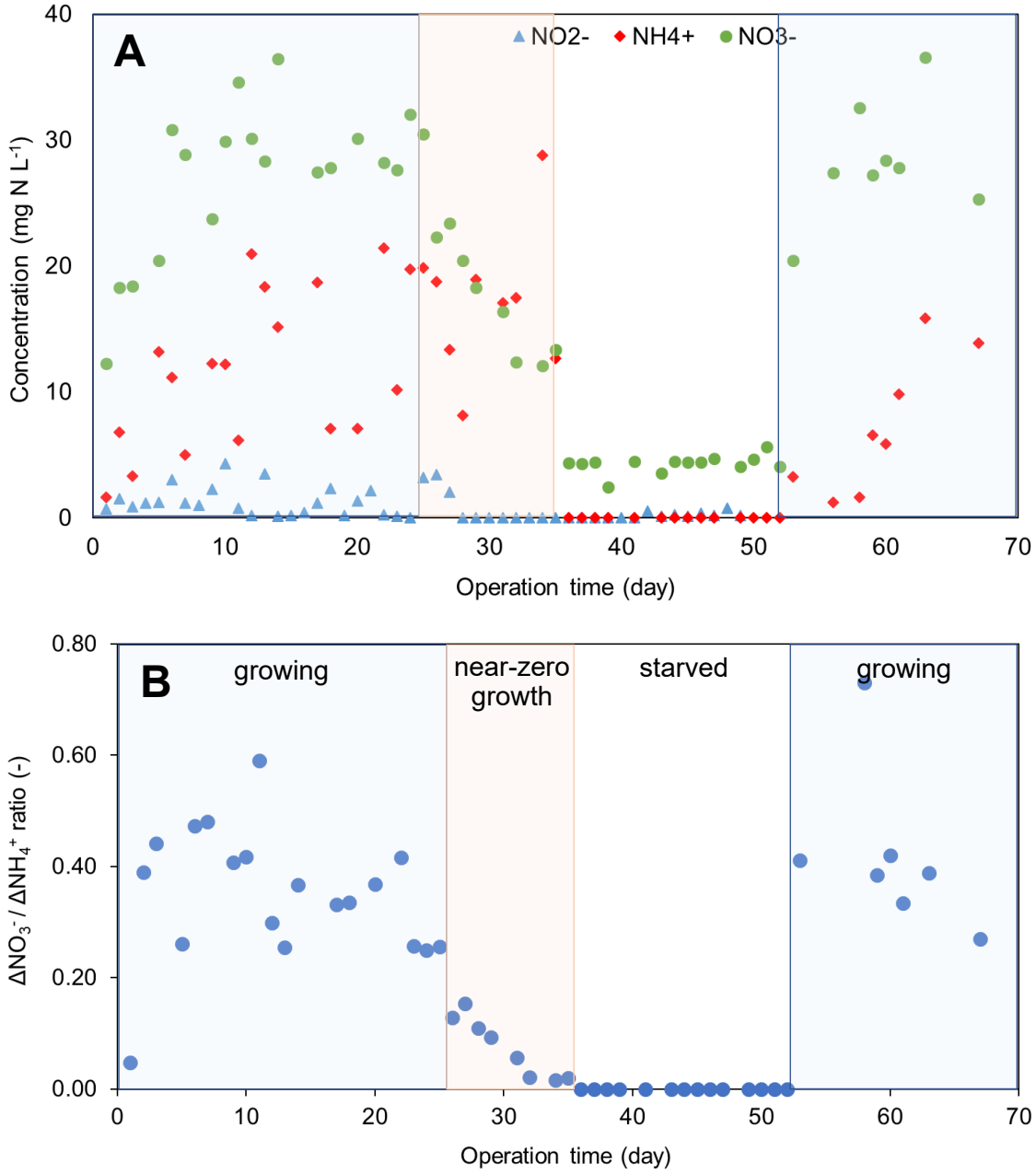


**Figure S4.** (**A**) Change in the concentrations of $NH_4^+$, $NO_2^-$, and $NO_3^-$ in MBR culture medium with time. (**B**) Change in the stoichiometric ratios of produced $NO_3^-$ and consumed $NH_4^+$ (0.355 ± 0.119 in the growing phase, 0.095 ± 0.079 in the near-zero growth phase, and 0.420 ± 0.147 in the 2nd growing phase ($P < 0.0001$)), showing that the reducing power (equivalent) for $CO_2$ fixation generated from $NO_2^-$ oxidation to $NO_3^-$ decreased under near-zero growth phase (Experimental Run-1).

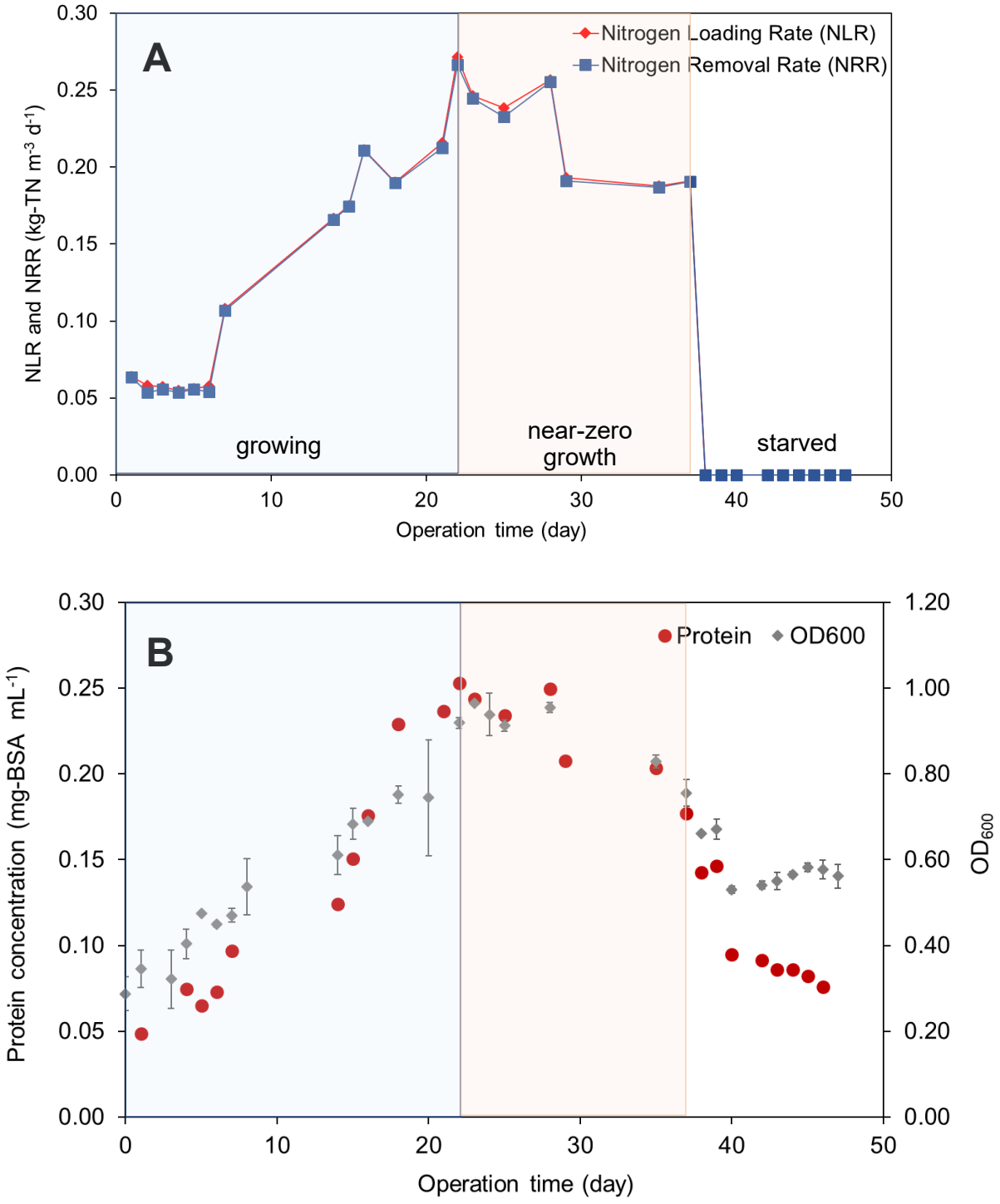


**Figure S5**. Time course of nitrogen ($NH_4^+$ and $NO_2^-$) loading rate (NLR) and removal rate (NRR) (**A**) and biomass concentration (protein and $OD_{600}$) (**B**) in a MRB during approx. 50 days of continuous operation (Experimental Run-2). Biomass cultures were collected for proteomic analysis in the growing (day 18), near-zero growth (day 31), and starved (day 50) phase, respectively. The error bars show SD of duplicate measurement.

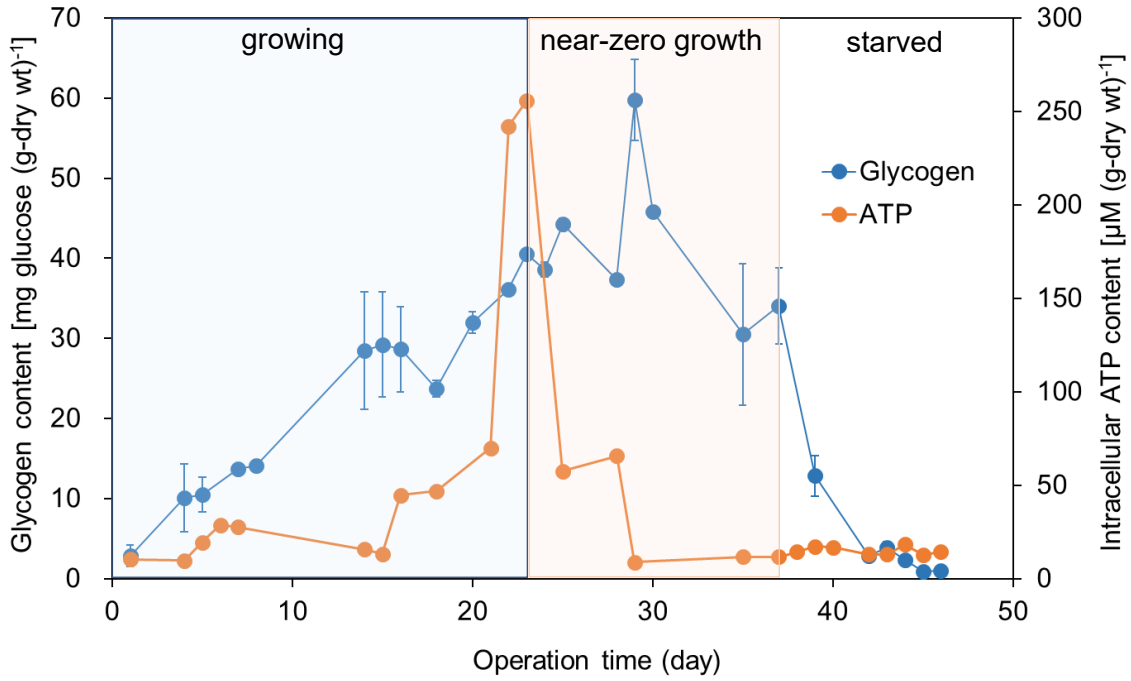


**Figure S6.** Change in intercellular glycogen content and ATP content in "*Ca*. B. sinica" with time (Experimental Run-2). Blue, orange, and white area indicate the growing phase, near-zero growth phase, and starved phase, respectively. The error bars represent the standard deviations of duplicate measurements. The error bars show SD of duplicate measurement.

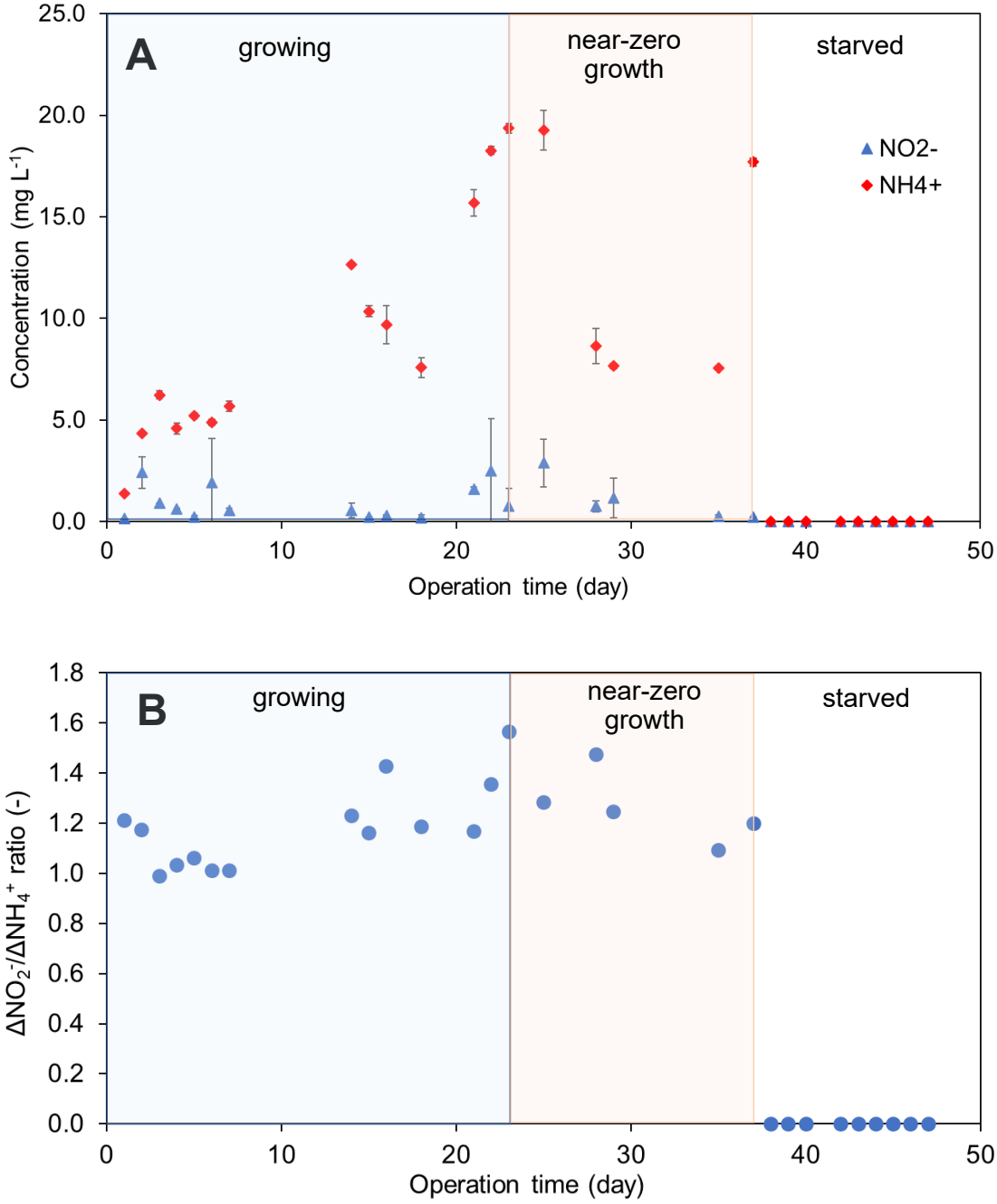


**Figure S7.** (**A**) Change in the concentrations of $NH_4^+$ and $NO_2^-$ in MBR culture medium with time. (**B**) Change in the stoichiometric ratio of produced $NO_2^-$ and consumed $NH_4^+$, showing that the reducing power (equivalent) for $CO_2$ fixation obtained from $NO_2^-$ oxidation to $NO_3^-$ decreased under near-zero growth phase. (Experimental Run-2) Blue, orange, and white area indicate the growing phase, near-zero growth phase, and starved phase, respectively. The error bars indicate the standard deviations of duplicate measurements. The error bars show SD of duplicate measurement.

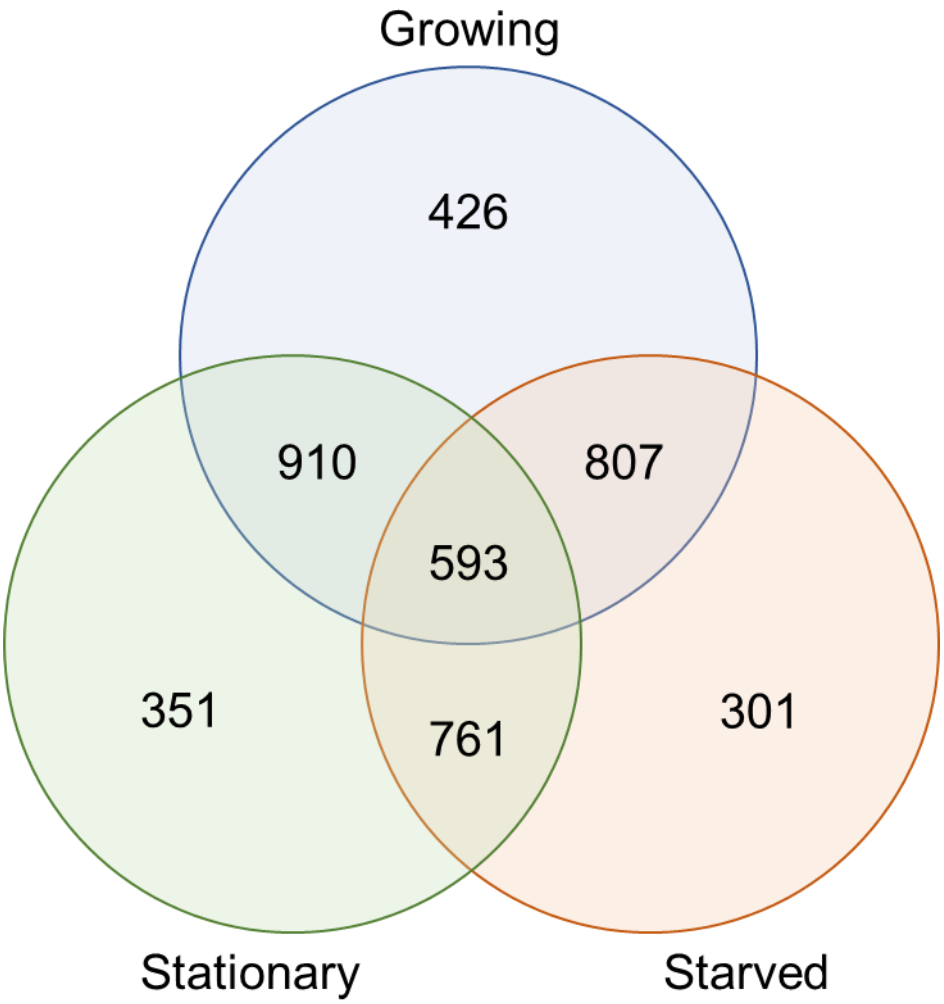


**Figure S8.** Venn diagram showing numbers of shared genes of "*Ca*. B. sinica" growing in three different growth conditions.